JOURNAL OF Materials CHEMISTRY

IR laser thermolytic conversion of disiloxanes to polyoxocarbosilane phase and silicon carbide

Nathalie Herlin-Boime,*[a] François Ténégal,[a]† Zdeněk Bastl,[b] Jan Šubrt,[c] Kristýna Jursíková,[d] Vratislav Blechta[d] and Josef Pola*[d]

[a]*Laboratoire Francis Perrin (CEA-CNRS URA-2453) DSM - Service des Photons, Atomes et Molécules-Bat 522, CEA Saclay, 91191 Gif sur Yvette Cedex, France. E-mail: herlin@drecam.cea.fr*
[b]*J. Heyrovský Institute of Physical Chemistry, Academy of Sciences of the Czech Republic, 18223 Prague 8, Czech Republic*
[c]*Institute of Inorganic Chemistry, Academy of Sciences of the Czech Republic, 25068 Řež near Prague, Czech Republic*
[d]*Laser Chemistry Group, Institute of Chemical Process Fundamentals, Academy of Sciences of the Czech Republic, 165 02 Prague 6, Czech Republic*

Received 13th December 2001, Accepted 18th February 2002
First published as an Advance Article on the web 8th March 2002

Continuous-wave CO_2 laser irradiation into gaseous methyldisiloxanes $[(CH_3)_nH_{3-n}Si]_2O$ (n = 2,3) at 1000 °C yields nanosized Si/C/O–carbon composites and at 2000 °C affords SiC–Si/C/O–carbon composites. The results demonstrate the feasibility of the direct production of silicon carbide from disiloxanes and suggest that the laser-induced homogeneous thermolysis of disiloxanes to SiC can be a preferred alternative to the earlier reported conventional thermolysis of specially synthesized polysiloxanes.

Introduction

Silicon oxycarbide materials with high-temperature strength and chemical stability have recently been paid much attention. Their synthesis was achieved by thermolytic conversion of oxygenated organosilicon precursors, mostly oligomeric and polymeric crosslinked siloxanes synthesized *via* the sol–gel route from alkoxysilanes (*e.g.*, ref. 1). The crosslinked polysiloxanes are suitable precursors to the Si/C/O phases, since their thermal degradation, dissimilarly to that of linear- and branched-chain polysiloxanes,[2] does not proceed through volatilization of cyclic oligomers.[3]

High-temperature pyrolysis of Si/C/O phases as well as that of crosslinked siloxane polymers can lead to the formation of silicon carbide,[1a,1b,1f,4] the key feature of obtaining SiC from the siloxanes being heating to above 1600 °C and having enough carbon to allow CO evolution (*e.g.*, ref. 4*a*,4*f*). The fact that the siloxanes can be converted into silicon carbide and carbon in controllable proportions makes them useful as binders for the sintering of silicon carbide monoliths.

We have reported on other, simpler approaches towards Si/C/O phases based on UV laser induced photolysis and IR laser thermolysis of gaseous organosilanes[5] (*e.g.*, disiloxanes)[5a–d] and on pyrolytic IR laser-interaction with an aerosol of ethoxy(methyl)silanes and hexamethyldisiloxane.[6] These approaches involve absorption of laser photons in a simple monomer, occur within a few milliseconds, and involve a multitude of decomposition and polymerization steps along with scrambling of SiO_xC_{4-x} moieties. They result in the formation of Si/C/O phases similar to those produced by high-temperature treatment of oligomeric and polymeric crosslinked siloxanes.[3]

The rules for the estimation of the Si/C/O ceramic composition from polymeric siloxane structure[7] as well as high-temperature chemistry of conversion of polysiloxanes to silicon carbide[4] have been reported.

As to the laser-induced production of Si/C/O materials, it is only known[6b] that the O content in them reflects that in the $(CH_3)_nSi(OC_2H_5)_{4-n}$ precursor. However, no information on whether ethoxy(methyl)silanes or disiloxanes can serve as simple precursors of silicon carbide is available.

In this paper we report on IR laser-interaction with an aerosol of 1,1,3,3-tetramethyldisiloxane and hexamethyldisiloxane. We reveal that the irradiation of both compounds at a low energy density yields similar nanometric Si/C/O–C composite powders, whereas irradiation at a high energy density results in the formation of nanometric Si/C/O–SiC–C composite powders with the relative SiC content depending on the precursor. The results demonstrate the feasibility of direct SiC production from disiloxanes.

Experimental

The laser irradiation experiments were performed in a set-up consisting of a precursor reservoir, a reaction chamber and a powder collector as described elsewhere.[8] Briefly, the liquid precursor (1,1,3,3-tetramethyldisiloxane (TMDSO) or hexamethyldisiloxane (HMDSO)) was placed in a glass jar, heated at 80 °C and introduced orthogonally to the laser beam in gaseous form using an Ar gas carrier (total pressure 740 Torr) through glass tubing (diameter 12 mm) at a flow rate of 100 ml min^{-1}. Nanopowders are formed by homogeneous nucleation and growth in the interaction zone that manifests itself by flame. The PRC Oerlikon continuous wave (CW) CO_2 laser was tuned to the 9 P (12) line (9.49 μm). Both disiloxanes (Aldrich) are good absorbers of the laser radiation, since they possess strong infrared active ν(SiOSi) wide bands at 9.31 (HMDSO) and 9.29 (TMDSO) μm. The laser beam was unfocused or focused (a lens with a focal length of 50 cm). The residence time in the laser beam for the unfocused and focused

†Present address: DRT-SEMM, CEA Saclay, 91191 Gif sur Yvette Cedex, France.

 DOI: 10.1039/b111364j

laser beam was estimated as *ca.* 20 and 2 ms, respectively. The flame temperature was measured by an optical pyrometer.

The collected powders were analysed for their properties by several methods.

The morphology was characterized by transmission electron microscopy (TEM) and Brauner, Emmet and Teller (BET) surfaces. TEM photomicrographs were obtained using a Philips 201 transmission electron microscope. BET surfaces of the powders were measured using a Micromeritics Flowsorb 2300 instrument

FTIR spectra of the powders in KBr pellets were obtained using a PerkinElmer 2000 spectrometer.

The X-ray photoelectron spectroscopy (XPS) and X-ray excited Auger electron spectroscopy (XAES) analyses were carried out using a VG ESCA 3 Mk II electron spectrometer and Al Kα (1486.6 eV) radiation. The spectra of Si KLL electrons were excited by Bremsstrahlung radiation. The powders were sputtered with argon ions under mild conditions (E = 5 keV, I = 20 μA, t = 5 min) to remove possible superficial contamination. Calculation of the concentrations of elements was accomplished by correcting the photoelectron peak intensities for their cross-sections[9] and accounting for the dependence of the analyser transmission and electron inelastic mean free paths on their kinetic energies.[10] The values for the binding energies were measured with an accuracy of $\pm$0.2 eV and the estimated error of the determined elemental concentrations was $\pm$10%.

X-ray diffraction diagrams of the powders were obtained on a Philips APD 1700 diffractometer at Cu Kα radiation.

Solid state MAS (magic angle spinning) and cross polarization (CP) MAS NMR were conducted on a Bruker DSX200 NMR spectrometer in 4 mm or 7 mm broadband probe. ^{13}C and ^{29}Si were externally referenced to the carbonyl line of glycine (δ = 176.03) and to the M unit line of M8Q8 (δ = 11.5), respectively. About 2000 scans were acquired for each ^{29}Si MAS spectrum with a spinning speed of 1500 Hz and a relaxation time delay of 30 s. ^{29}Si CP MAS spectra acquisitions required from 1000 to 5000 scans, the spinning speed chosen was 1500 Hz, the relaxation delay 6 s and CP delay 5 ms. ^{13}C CP MAS were recorded by about 11000 scans, a spinning speed of 3500 Hz and a CP delay time of 2 ms.

The Raman spectra were recorded on a PC-controlled spectrometer coupled with a photomultiplier operating in the photon counting mode. The exciting beam of an Ar-ion laser was defocused to diminish the heating of the samples.

Results and discussion

The CW CO_2 laser irradiation into gaseous $[(CH_3)_nH_{3-n}Si]_2O$ (n = 2,3) disiloxanes yields solid powders whose properties depend on the irradiating conditions. Typical experimental parameters and characterization results are compiled in Table 1.

Typical duration of the irradiation experiments was longer than 1 h with yields (produced powder/depleted precursor) in the range of 30–70%. The powder production was higher for TMDSO than for HMDSO and correlated with the amount of precursor carried in the reaction zone.

Flame temperature measurements clearly show that focusing the laser beam allows the temperature to increase. The powders produced with the focused and unfocused laser beam geometry possess similar, with one exception, specific surface areas.

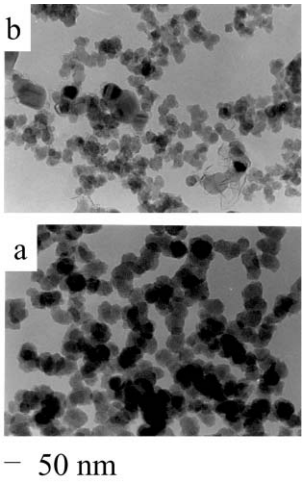

Fig. 1 TEM images of powders from TMDSO (unfocused (a) and focused (b) laser beam).

Properties of powders

With the unfocused laser beam, the stoichiometry deduced from XPS analysis (Table 1) of the powders from HMDSO and TMDSO is very similar: both powders maintain the Si : O ratio of their precursors and are poorer in carbon than their precursors.

With the focused laser beam, the stoichiometry of the powders from HMDSO and TMDSO differs: the powder from HMDSO shows the same Si : O ratio as the HMDSO precursor and that from TMDSO has the Si : O ratio significantly increased compared with the TMDSO precursor. These powders contain more carbon than those obtained with the unfocused radiation and the carbon content in them reflects the carbon content in their precursors.

The analyses given below reveal that the powders are composed of different species whose nature is dependent on the laser beam geometry and not on the precursor structure.

Electron microscopy. All the samples exhibit similar morphology and appear to be composed mainly of grains of round shape more or less agglomerated in a chain-like manner. The size of the grains is in the range 40–50 nm for the samples obtained with the unfocused radiation, whereas that of those produced with the focused radiation ranges between *ca.* 20–30 nm. Fig. 1 presents TEM images of the samples obtained from TMDSO with an unfocused and focused laser beam. The smaller size in the latter case is related to the shorter residence time in the laser beam. Fig. 1b allows the features of the typical of powders obtained from both precursors to be seen with the focused laser beam: crystallized particles and elongated structures similar to carbon ribbons.

FTIR absorption spectra. The FTIR spectra of the powders obtained with the unfocused laser beam (Fig. 2a,b) possess two

Table 1 Laser synthesis of nanopowders from disiloxanes[a]

Disiloxane precursor	Laser beam	T/°C	Disiloxane consumption/g h^{-1}	Powder yield/g h^{-1}	Conversion efficiency[b] (%)	XPS analysis	Powder BET surface/m^2 g^{-1}
HMDSO	Unfocused	910	2.9	1.0	34	$Si_1C_{0.85}O_{0.53}$	110
HMDSO	Focused	2000	2.9	1.6	55	$Si_1C_{1.61}O_{0.48}$	>270
TMDSO	Unfocused	1050	11.2	7.8	70	$Si_1C_{0.83}O_{0.45}$	125
TMDSO	Focused	2000	11.4	6.7	59	$Si_1C_{1.18}O_{0.23}$	130

[a]Conditions in Experimental. [b]As powder yield (g h^{-1})/disiloxane consumption (g h^{-1}).

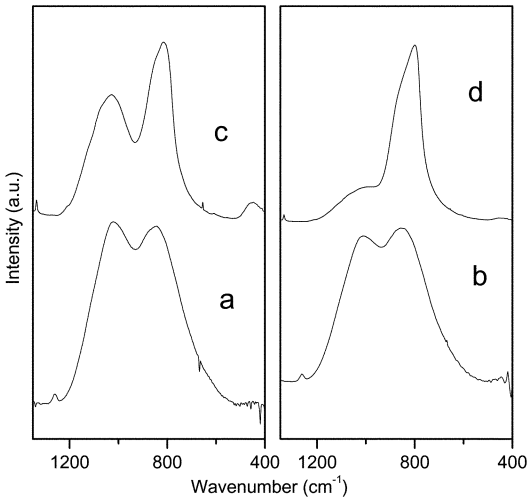

Fig. 2 FTIR absorption spectra of powders from HMDSO (unfocused (a) and focused (c) laser beam) and from TMDSO (unfocused (b) and focused (d) laser beam).

broad bands at 1020 and 843 cm^{-1} (powder from HMDSO) and at 1008 and 855 cm^{-1} (powder from TMDSO), which are of about equal absorbance and attributed to ν(Si–O) and ν(Si–C) vibrations. They also contain very weak bands at 1260 cm^{-1} and (not shown) 2180 cm^{-1}, which are, respectively, due to $\delta(CH_3Si)$ and ν(Si–H) vibrations. The former band indicates an incomplete decomposition of the precursors.

The FTIR spectra of the powders produced with the focused laser beam (Fig. 2c,d) have different patterns: that of the powder from HMDSO consists of absorption bands due to ν(Si–O) (1066 cm^{-1}) and ν(Si–C) (840 cm^{-1}) vibrations with a relative absorbance ratio $A_{\nu(Si-C)}:A_{\nu(Si-O)} = 1.4$, whereas that of the powder from TMDSO has just one broad ν(Si–C) band at 821 cm^{-1} with only a ν(Si–O) shoulder at *ca.* 1050 cm^{-1}. Neither of them possesses a contribution from the $\delta(CH_3Si)$ vibration.

XPS and XAES spectra. The Si(2p) core level binding energies of the powders produced using the unfocused laser beam (102.8 $\pm$ 0.2 eV for the powder from HMDSO and 102.4 $\pm$ 0.2 eV for the powder from TMDSO, Fig. 3b,d) fall into the range of values published for polyoxocarbosilanes.[11]

The Si(2p) spectra of the powders produced using the focused laser beam (Fig. 3a,c) can be decomposed in two components (located at 102.4 and 100.6 eV for the powder from HMDSO and 102.1 and 100.2 eV for the powder from

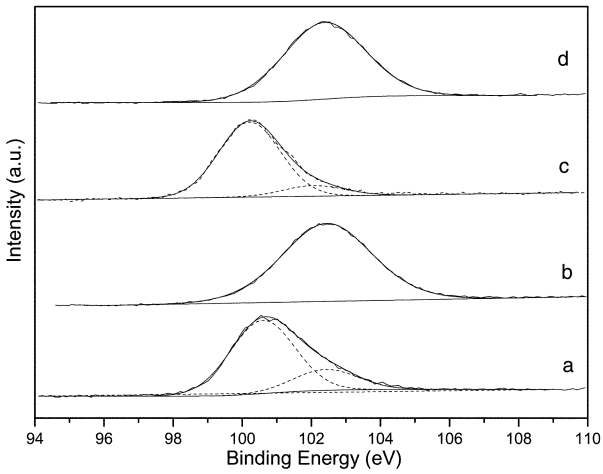

Fig. 3 Si(2p) core level spectra of powders from HMDSO (focused (a) and unfocused (b) laser beam) and from TMDSO (focused (c) and unfocused (d) laser beam).

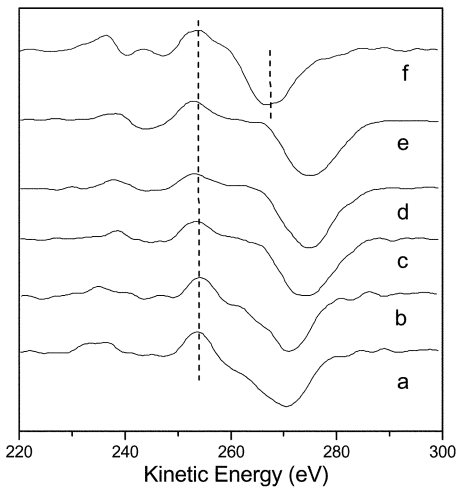

Fig. 4 C KLL X-ray excited derivative Auger spectra of powders from an unfocused (HMDSO (a) and TMDSO (b)) and a focused (HMDSO (c) and TMDSO (d)) laser beam and of graphite (e) and diamond (f).

TMDSO), which can be assigned[11] to an Si/C/O arrangement and silicon carbide, respectively. The presence of SiC is further supported by the value determined for the Si Auger parameter (1714.5 eV, defined as the sum of the Si(2p) core level binding energy and the kinetic energy of the Si KLL Auger electrons) and the content of Si in SiC in the sputtered powder surface layers is $\sim$70%. The presence of SiC is in agreement with the IR analysis presented above.

The carbon (sp^2/sp^3) hybridization ratio can be estimated using the energy difference between the most positive maximum and the most negative minimum of the C KLL derivative Auger spectra.[12] A linear relationship between this separation and the (sp^2/sp^3) ratio has been suggested.[12] The C KLL derivative spectra of the powders (Fig. 4) and their comparison with those obtained for diamond and graphite[12] confirm that both powders produced under the unfocused laser beam contain C(sp^3) and C(sp^2) atoms in a *ca.* 1 : 1 ratio, whereas the spectra of both powders obtained under the focused laser beam are dominated by the presence of C(sp^2) atoms in graphitic form, which is compatible with the presence of elongated structures attributed to aromatic carbon in the TEM images.

XRD spectra. The XRD pattern of the powders obtained under unfocused radiation indicates an amorphous state (Fig. 5a,b) whereas that of the powders obtained under the focused radiation (Fig. 5c,d) displays typical peaks at 35°, 60° and 72° belonging to β-SiC microcrystals. This is in good agreement with IR and XPS measurements.

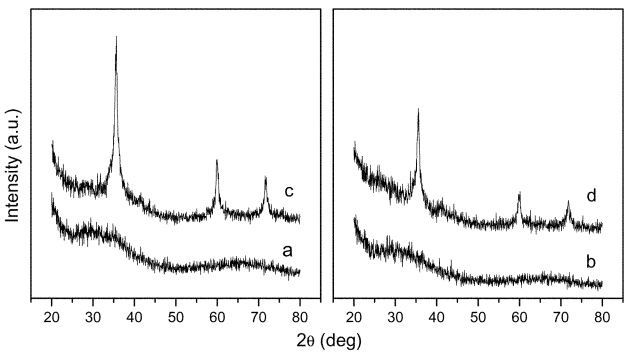

Fig. 5 XRD spectra of powders from HMDSO (unfocused (a) and focused (c) laser beam) and from TMDSO (unfocused (b) and focused (d) laser beam).

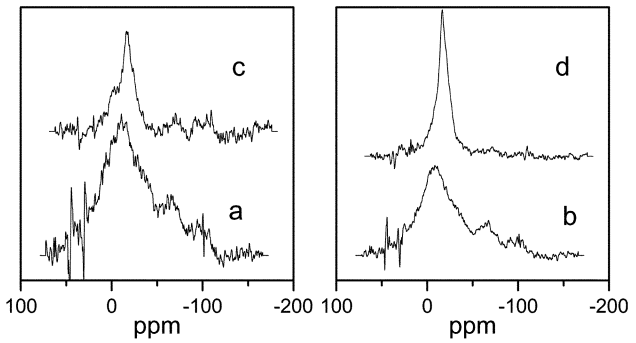

Fig. 6 ^{29}Si MAS spectra of powders from HMDSO (unfocused (a) and focused (c) laser beam) and from TMDSO (unfocused (b) and focused (d) laser beam).

NMR spectra. The ^{29}Si MAS NMR spectra for the powders obtained under the unfocused radiation from HMDSO (Fig. 6a) and TMDSO (Fig. 6b) consist of a broad band at 20–40 ppm and two other bands centered at −65 ppm and 100 ppm. The broad band covers the region of M (SiC_3O, 10–0 ppm), M_H ($SiHC_2O$, −6–−8 ppm), X (SiC_4, 0–−15 ppm) and D (SiC_2O_2, −19–−22 ppm) units, of D units in strained ring structures (*ca.* −35 ppm) and of D_H ($SiHCO_2$, −32–−37 ppm) unit. The other two bands are due to T ($SiCO_3$, −55–−64 ppm) and Q (SiO_4, −95–−115 ppm) structural units.[13,14a]

The ^{29}Si MAS NMR spectra for the powders obtained under the focused radiation from HMDSO (Fig. 6c) and TMDSO (Fig. 6d) are dominated by a band centred at *ca.* −16 ppm, which we assign[14b] to β-SiC. This assignment is in agreement with the observations reported above and is supported by the ^{29}Si CP MAS NMR spectra not showing any signal, which indicates the absence of protons.

The ^{13}C CP MAS NMR spectra of the powders (Fig. 7) show two signals, one at +20–−10 ppm with a sharp maximum at 0 ppm belonging to $(CH_3)_nSi$ (or possibly[15,16] to tetrahedral SiC_4, $(Si)CH_2(Si)$, –C–CH_2–Si, or Si–CH_2–CH_2–Si units), together with a broad band at 120–150 ppm, which is characteristic of sp^2 aromatic carbon. Almost unobserved signals for the powder from TMDSO with a focused beam (Fig. 7c) seem to indicate a very low content of both aromatic and aliphatic carbons with proximal protons.

Raman spectra. Raman spectra (Fig. 8) give supporting evidence on the forms of the incorporated carbon. They reveal that both powders produced under the unfocused laser beam conditions contain strongly disordered carbon having a characteristic bifurcated band with maxima at 1362 cm^{-1} (band D) and 1570 cm^{-1} (band G). Both powders obtained with the focused laser beam show well separated D (1338 cm^{-1}) and G (1574 cm^{-1}) bands characteristic of polycrystalline or microcrystalline graphite. We note the occurrence of a two phonon band (2400–3300 cm^{-1}) and a small shift of this and the D band to lower wavenumbers, which is likely due[17] to incorporation of SiC-like structures.

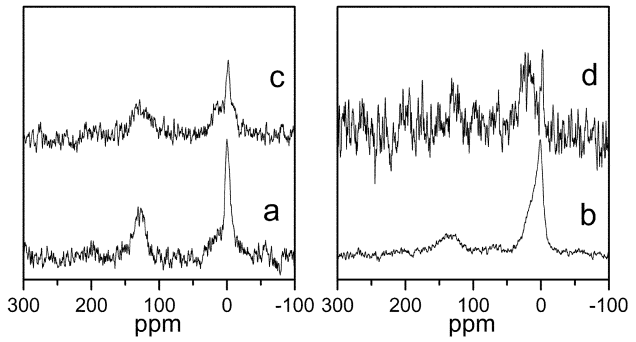

Fig. 7 ^{13}C NMR spectra of powders from HMDSO (unfocused (a) and focused (c) laser beam) and from TMDSO (unfocused (b) and focused (d) laser beam).

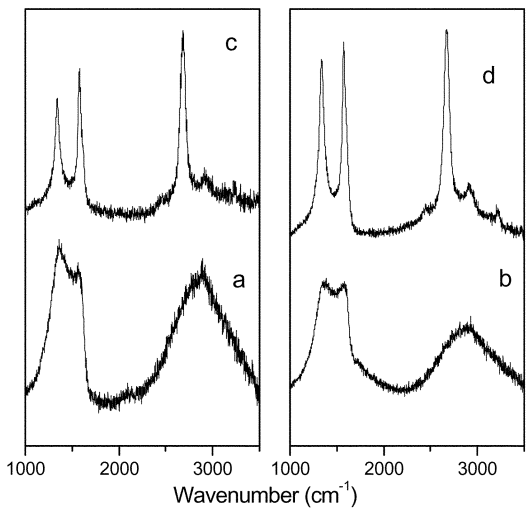

Fig. 8 Raman spectra of powders from HMDSO (unfocused (a) and focused (c) laser beam) and from TMDSO (unfocused (b) and focused (d) laser beam).

The different analyses reported here reveal that the properties of the powders produced with the focused and unfocused laser beam geometry are different.

The powders produced from HMDSO and TMDSO under the unfocused radiation at *ca.* 1000 °C have their stoichiometry *ca.* $Si_1C_{0.8}O_{0.5}$ and are composites of carbon and polyoxocarbosilanes. The contained polyoxocarbosilanes are poorer in carbon and hydrogen than their precursors, but contain some $CH_3(Si)$ groups due to incomplete decomposition of the precursor. Although these materials maintain the Si : O ratio of their precursors, they incorporate different $SiO_xC(H)_{4-n}$ configurations as observed previously[6] for powders synthesized from HMDSO used as an aerosol.

The powders obtained by the focused irradiation into HMDSO and TMDSO at *ca.* 2000 °C are composites of polyoxocarbosilane, graphite and crystalline silicon carbide. Due to the higher temperature, the polyoxocarbosilanes do not contain $CH_3(Si)$ groups. The stoichiometry of these composites—$Si_1C_{1.61}O_{0.48}$ (from HMDSO) and $Si_1C_{1.18}O_{0.23}$ (from TMDSO)—is different and the powder from HMDSO contains less SiC even though HMDSO is richer in C than TMDSO.

Chemistry involved

The high temperatures make possible a number of decomposition steps for the disiloxanes. At 1000 °C, there is enough energy for cleavage of all the Si–C (*ca.* 370 kJ mol^{-1}), C–H (*ca.* 410 kJ mol^{-1}), Si–H (*ca.* 380 kJ mol^{-1}) and Si–O (*ca.* 530 kJ mol^{-1}) bonds and also for inducing three-center elimination of silylenes and carbenes (∼250–300 kJ mol^{-1}, refs. 18–20). We presume that the primary steps are Si–C and Si–H bond homolysis yielding Si-centered radicals along with 1,1-[CH_4] extrusions[21,22] yielding silylenes. The Si-centered radicals can decompose into[5] very reactive silanones

$$(CH_3)_{n-1}H_{3-n}Si^{\bullet}–OSi(CH_3)_nH_{3-n} \rightarrow (CH_3)_{n-1}H_{3-n}Si{=}O + {}^{\bullet}Si(CH_3)_nH_{3-n}$$

which undergo polymerization,

$$n(CH_3)_nH_{2-n}Si{=}O \rightarrow –[(CH_3)_nH_{2-n}Si–O]_n–$$

or take part, together with silylenes, in agglomeration reactions

through insertion of silanones into the Si–O and of silylenes into the Si–H bonds of intermediates. These reactions yield various polyoxocarbosilanes, which undergo Si–C/Si–O and Si–H/Si–O scrambling to different $SiC(H)_xO_{4-x}$ configurations.[1b,4d,23] The observed carbon phases are evidently produced *via* a number of combination and dehydrogenation steps of the initially liberated methyl radicals.

At 2000 °C, the above-assumed reactions are accompanied by formation of silicon carbide. There are two possible routes for its formation, namely Si–O/Si–C redistribution yielding SiC_4 units,[23] and carbothermic reduction[24] of the polyoxocarbosilane network with excess of free carbon phase.[1b,4d] Both routes are already accessible at *ca.* 1400 °C. The higher temperature decreases the content of hydrogenated structures and induces formation of graphite. The higher content of carbon in these deposits indicates that methyl units were more efficiently carbonized (and obviously yielded less volatile hydrocarbons). The higher content of SiC from TMDSO reveals that its formation is enhanced by the presence of the (Si)–H bonds.

Inferences

We reveal that CW CO_2 laser irradiation into hexamethyldisiloxane and 1,1,3,3-tetramethyldisiloxane at 1000 °C (unfocused laser beam) yields nanosized Si/C/O–carbon composites and that that irradiation at 2000 °C (focused laser beam) affords SiC–Si/C/O–graphite composites.

The results demonstrate for the first time that direct production of silicon carbide is feasible from disiloxanes, which can make the above-reported approach preferable to those using conventional thermolysis of specially synthesized oligomeric and polymeric crosslinked siloxanes.[1] The above-reported procedure for SiC production can easily be scaled-up[6] by using a higher laser power and a faster Ar–disiloxane flow to yield larger amounts of nanoparticles by a continuous method.

The results add to our studies of IR laser thermolytic conversion of disiloxanes to polyoxocarbosilane phases using pulsed IR laser irradiation[5] into gaseous disiloxanes, and of CW laser-interaction with disiloxane aerosol[6] and show that CW high energy density irradiation is more effective for formation of silicon carbide than high energy laser irradiation delivered[5a,5d,25] in short pulses.

Polyoxocarbosilane and carbon phases produced at 1000 °C are likely intermediates to SiC and graphite phases produced at 2000 °C; this makes them suitable[4d] binder materials for ceramic powders in the preparation of sintered ceramic monoliths.

Acknowledgement

This work was supported by bilateral co-operation between the Czech Republic and France (Barrande program) and by the Ministry of Education, Youth and Sport of the Czech Republic (grant no. 2001-010-1). The authors thank Dr. I. Gregora for the Raman spectroscopy measurements and Dr. M. Mayne for the XRD analyses.

References

1 (*a*) F. Babonneau, K. Thorne and J. D. Mackenzie, *Chem. Mater.*, 1989, **1**, 554; (*b*) G. D. Soraru, G. D'Andrea, R. Campostrini, F. Babonneau and G. Mariotto, *J. Am. Ceram. Soc.*, 1995, **78**, 379 and references cited therein; (*c*) L. Bois, J. Maquet, F. Babonneau, H. Mutin and D. Bahloul, *Chem. Mater.*, 1994, **6**, 796; (*d*) R. A. Mantz, P. F. Jones, K. P. Chaffee, J. D. Lichtenhan, J. W. Gilman, I. M. K. Ismail and M. J. Burmeister, *Chem. Mater.*, 1996, **8**, 1250; (*e*) G. D. Soraru, Q. Liu, L. V. Interrante and T. Apple, *Chem. Mater.*, 1998, **10**, 4047; (*f*) E. Breval, M. Hammond and C. G. Pantano, *J. Am. Ceram. Soc.*, 1994, **77**, 3012.

2 (*a*) T. H. Thomas and T. C. Kendrick, *J. Polym. Sci.*, 1970, **8**, 1823; (*b*) J. M. Nielsen, *J. Appl. Polym. Sci., Appl. Polym. Symp.*, 1979, **35**, 223.

3 A. M. Wilson, G. Zank, K. Euguchi, W. Xiing, B. Yates and J. R. Dahn, *Chem. Mater.*, 1997, **9**, 1601.

4 (*a*) D. A. White, S. M. Oleff, R. D. Boyer, P. A. Budinger and J. R. Fox, *Adv. Ceram. Mater.*, 1987, **2**, 53; (*b*) F. I. Hurwitz, P. Heimann, S. C. Farmer and D. M. Hembree, *J. Mater. Sci.*, 1993, **28**, 6622; (*c*) W. H. Atwell, G. T. Burns and C. K. Saha, *US Pat.*, 1989, 4 888 376; (*d*) G. T. Burns, R. B. Taylor, Y. Xu, A. Zangvil and G. A. Zank, *Chem. Mater.*, 1992, **4**, 1313.

5 (*a*) J. Pola, M. Urbanova, Z. Bastl, J. Subrt and P. Papagiannakopoulos, *J. Mater. Chem.*, 2000, **10**, 1415; (*b*) J. Pola, A. Ouchi, J. Subrt, Z. Bastl, M. Sakuragi, A. Galiková and A. Galík, *Adv. Mater.*, 2001, **7**, 19; (*c*) J. Pola, A. Galíková, A. Galík, V. Blechta, Z. Bastl, J. Šubrt and A. Ouchi, *Chem. Mater.*, 2002, **14**, 144; (*d*) M. Urbanová, Z. Bastl, J. Šubrt and J. Pola, *J. Mater. Chem.*, 2001, **11**, 1557; (*e*) J. Pola, J. Vítek, Z. Bastl and J. Šubrt, *J. Organometal. Chem.*, 2001, **640**, 170.

6 (*a*) Y. El Kortobi, J. B. d'Espinose de la Cailerie, A. P. Legrand, X. Armand, N. Herlin and M. Cauchetier, *Chem. Mater.*, 1997, **9**, 632; (*b*) N. Herlin, X. Armand, E. Musset, H. Martinengo, M. Luce and M. Cauchetier, *J. Eur. Ceram. Soc.*, 1996, **16**, 1063.

7 D. R. Bujalski, S. Grigoras, W. L. Lee, G. M. Wieber and G. A. Zank, *J. Mater. Chem.*, 1998, **8**, 1427.

8 (*a*) M. Cauchetier, O. Croix, N. Herlin and M. Luce, *J. Am. Ceram. Soc.*, 1994, **77**, 993; (*b*) M. Luce, N. Herlin, E. Musset and M. Cauchetier, *Nanostruct. Mater.*, 1994, **4**, 403.

9 J. H. Scofield, *J. Electron Spectrosc.*, 1976, **8**, 129.

10 M. P. Seah and W. A. Dench, *Surf. Interface Anal.*, 1979, **1**, 1.

11 C. D. Wagner, in *Practical Surface Analysis, Vol. 1, Auger and X-ray Photoelectron Spectroscopy*, ed. D. Briggs and M. P. Seah, Wiley, Chichester, 1994, p. 595.

12 J. M. Lascovich, R. Giorgi and S. Scaglione, *Appl. Surf. Sci.*, 1991, **47**, 17; S. T. Jackson and R. G. Nuzzo, *Appl. Surf. Sci.*, 1995, **90**, 195.

13 H. Marsmann, in *NMR Basic Principles and Progress*, ed. P. Diehl, E. Fluck and R. Kosfeld, Springer-Verlag, Berlin, 1981, vol. 17; K. Beshah, J. E. Mark and J. Ackerman, *J. Polym. Sci., Part B*, 1986, **24**, 1207.

14 (*a*) Q. Liu, W. Shi, F. Babonneau and L. V. Interrante, *Chem. Mater.*, 1997, **9**, 2434; (*b*) J. R. Guth and W. T. Petruskey, *J. Phys. Chem.*, 1987, **91**, 5361.

15 W. R. Schmidt, L. V. Interrante, R. H. Doremus, T. K. Trout, P. S. Marchetti and G. E. Maciel, *Chem. Mater.*, 1991, **3**, 257.

16 V. Belot, R. J. P. Corriu, D. Leclercq, P. H. Mutin and A. Vioux, *J. Non-Cryst. Solids*, 1992, **144**, 287.

17 M. Ramsteiner, J. Wagner, C. Wild and P. Koidl, *Solid State Commun.*, 1988, **67**, 15.

18 J. M. Jasinski and R. D. Estes, *Chem. Phys. Lett.*, 1985, **117**, 495.

19 J. M. Jasinski, R. Becerra and R. Walsh, *Chem. Rev.*, 1995, **95**, 1203.

20 S. W. Benson, *Thermochemical Kinetics*, Wiley, New York, 1976.

21 S. E. Rickborn, M. A. Ring, H. E. O'Neal and D. Coffey, *Int. J. Chem. Kinet.*, 1984, **16**, 289.

22 J. Pola and R. Taylor, *J. Organometal. Chem.*, 1993, **446**, 131 and references cited therein.

23 V. Belot, R. J. P. Corriu, D. Leclercq, P. H. Mutin and A. Vioux, *J. Mater. Sci. Lett.*, 1990, **9**, 1052; V. Belot, R. J. P. Corriu, D. Leclercq, P. H. Mutin and A. Vioux, *Chem. Mater.*, 1991, **3**, 127.

24 N. Klinger, E. L. Strauss and K. L. Komarek, *J. Am. Ceram. Soc.*, 1966, **49**, 369.

25 J. Kupčík, Z. Bastl, J. Šubrt, J. Pola, V. C. Papadimitriou, A. V. Prosmitis and P. Papagiannakopoulos, *J. Anal. Appl. Pyrol.*, 2001, **57**, 109.